

Supplementary Materials for Stabilizing electrochemical interfaces in viscoelastic liquid electrolytes

Shuya Wei, Zhu Cheng, Pooja Nath, Mukul D. Tikekar, Gaojin Li, Lynden A. Archer

Published 23 March 2018, *Sci. Adv.* **4**, eaao6243 (2018)

DOI: 10.1126/sciadv.aao6243

This PDF file includes:

- fig. S1. An illustration showing the lithium symmetric coin cell used for the *I-V* electrokinetic measurements.
- fig. S2. Electrokinetic characteristics of viscoelastic electrolytes as a function of measurement time.
- fig. S3. Linear sweep voltammetry as a function of PMMA concentration at a scan rate of 1 mV/s.
- fig. S4. Schematic drawing of the experimental setup used to perform the visualization experiment for electrodeposition.
- fig. S5. Tracer particle velocities in the Newtonian liquid electrolyte (EC/PC–1 M LiTFSI) and a representative viscoelastic electrolyte (4 wt % PMMA in EC/PC–1 M LiTFSI) as a function of voltage.
- fig. S6. Complex shear viscosity at 25°C for viscoelastic liquid electrolytes containing varying concentrations of PMMA.
- fig. S7. EIS measurements and analysis for viscoelastic electrolytes with different polymer concentrations.
- fig. S8. Depth-profiling XPS spectra of a lithium metal surface after electrodeposition for 1 hour at a current density of 1 mA/cm².
- fig. S9. Photographic images showing evolution of various metal electrode/electrolyte interfaces during electrodeposition.
- table S1. Measured Li⁺ transference numbers and calculated limiting current densities [in the optical cell (*J*₁) and O-ring coin cell (*J*₂)] for electrolytes used in the study.

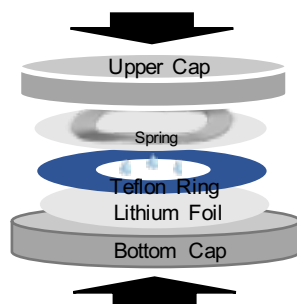


fig. S1. An illustration showing the lithium symmetric coin cell used for the *I-V* electrokinetic measurements. Cells were maintained in the “stable configuration” in which Li^+ ions are produced by oxidation at the lower (bottom) electrode and reduced at the upper (top) metal electrode.

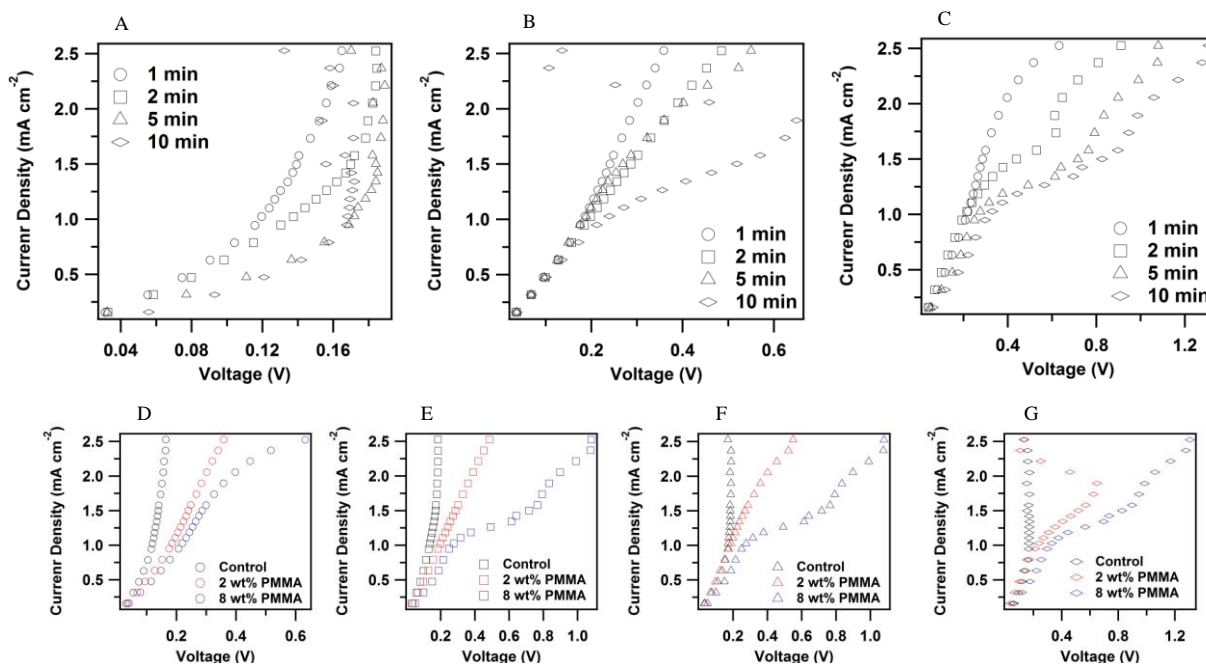


fig. S2. Electrokinetic characteristics of viscoelastic electrolytes as a function of measurement time. (A, B and C) Current-voltage curves for electrolytes with (A) no PMMA, (B) 2wt% PMMA and (C) 8wt% PMMA plotted as a function of time used for each current step. (D, E, F, G) Current-voltage curves of the electrolyte with different concentrations of PMMA showing result of varying the time for each current step: (D) 1 min, (E) 2 min, (F) 5 min and (G) 10 min for each current step.

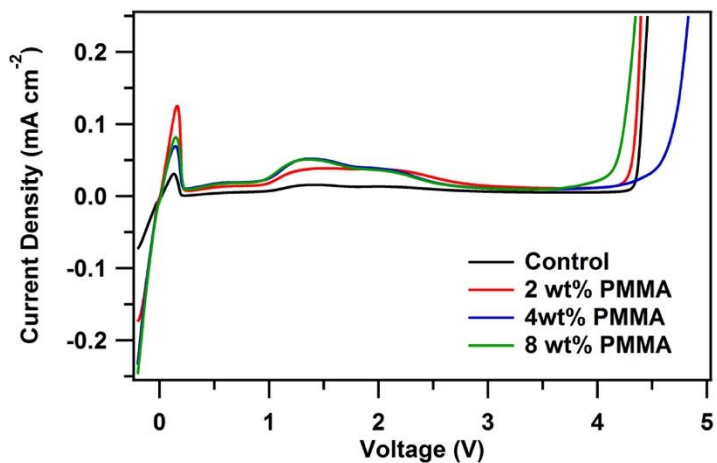


fig. S3. Linear sweep voltammetry as a function of PMMA concentration at a scan rate of 1 mV/s. The prominent current peak in the range -0.2 to 0.2 V associated with Li stripping is seen to become slightly more prominent as the polymer concentration in the electrolytes is increased, but to remain centered at the same voltage.

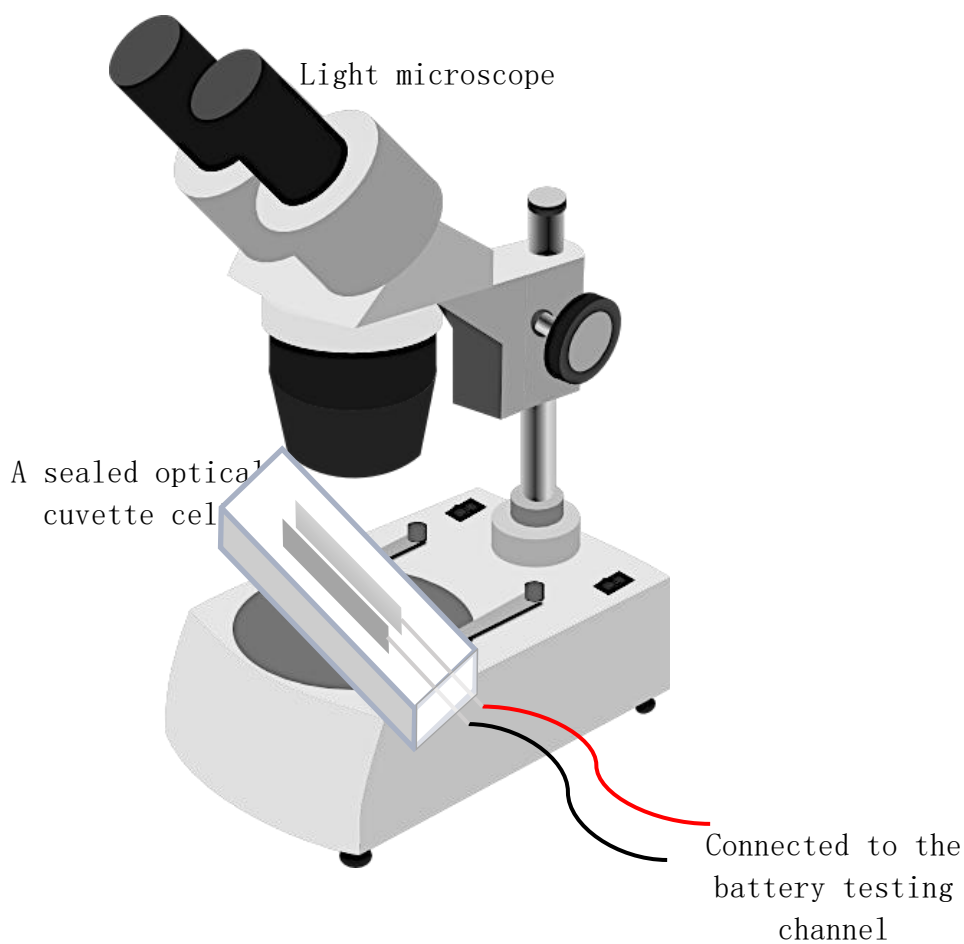


fig. S4. Schematic drawing of the experimental setup used to perform the visualization experiment for electrodeposition.

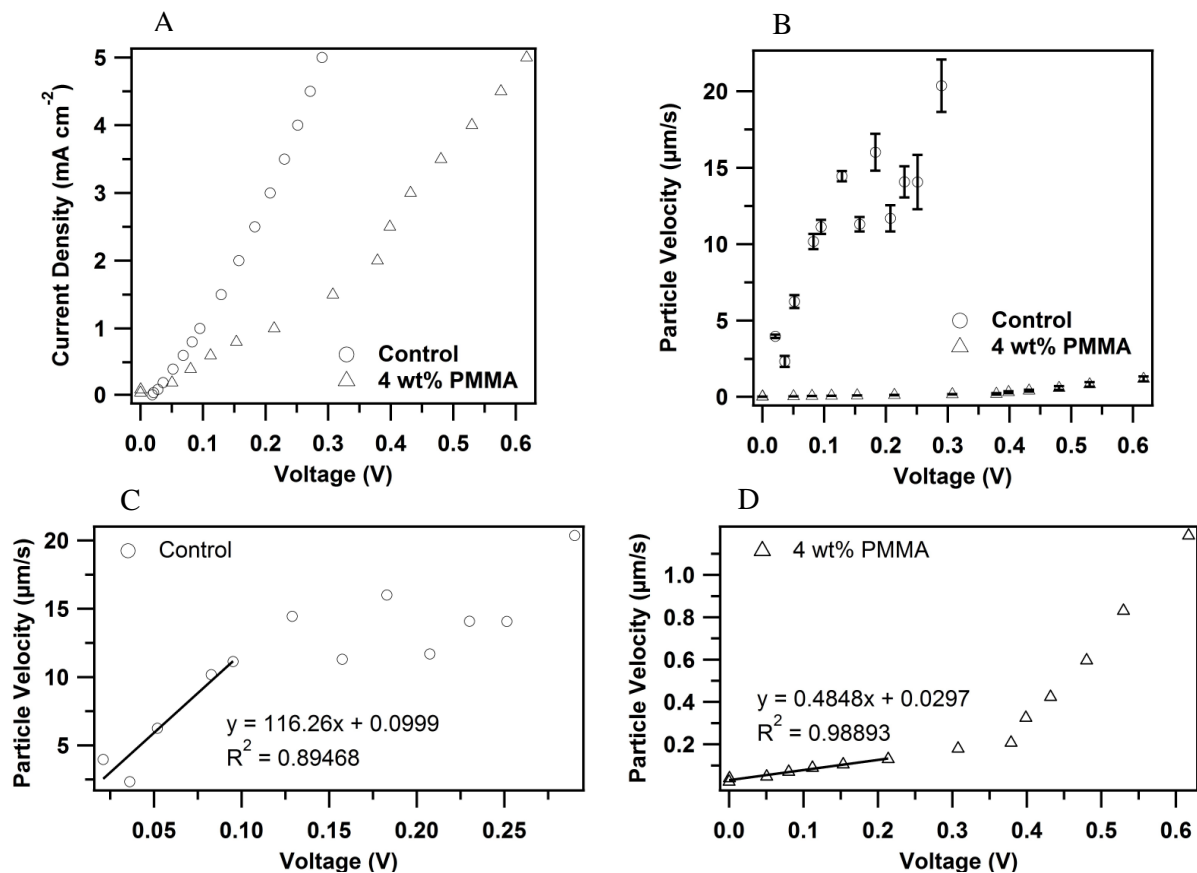


fig. S5. Tracer particle velocities in the Newtonian liquid electrolyte (EC/PC–1 M LiTFSI) and a representative viscoelastic electrolyte (4 wt % PMMA in EC/PC–1 M LiTFSI) as a function of voltage. (A) Current-Voltage curves of the electrolytes with and without PMMA in the electrolyte. (B) Tracer velocity as a function of voltage. (C), (D) Respective, linear analysis of the flow velocity at low current densities for the control (no PMMA) and viscoelastic liquid electrolytes.

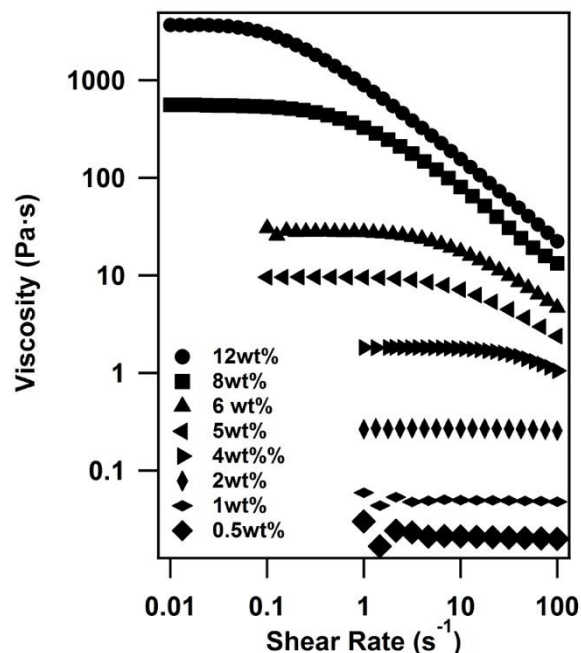


fig. S6. Complex shear viscosity at 25°C for viscoelastic liquid electrolytes containing varying concentrations of PMMA.

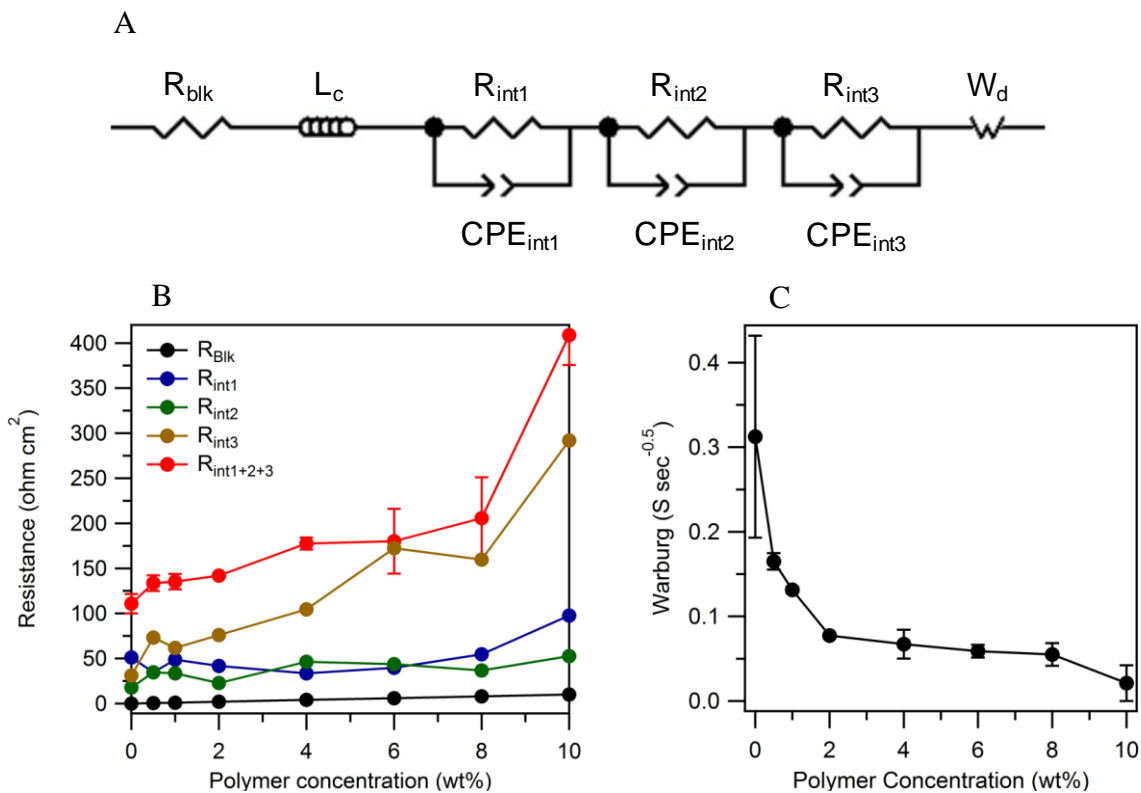
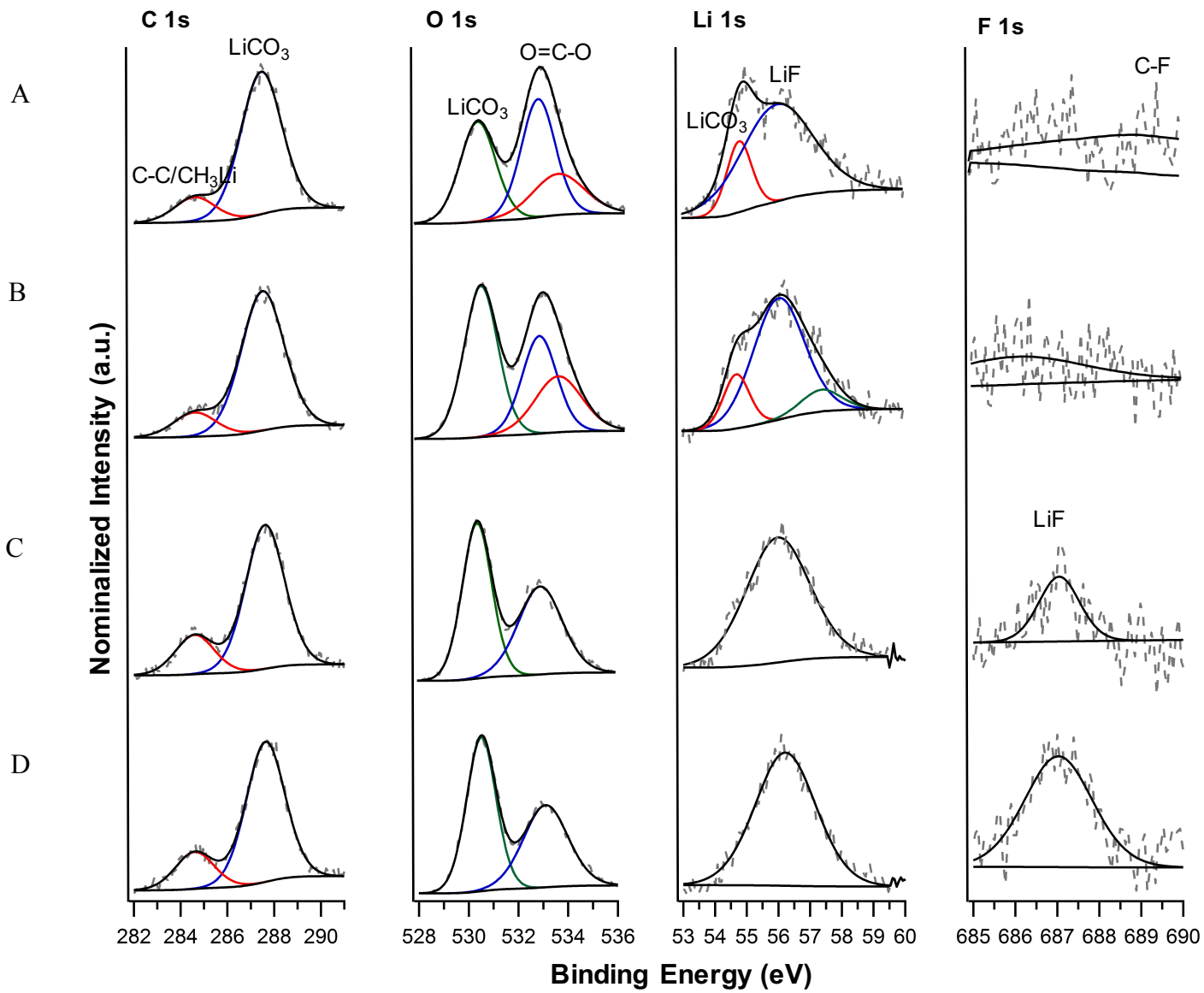


fig. S7. EIS measurements and analysis for viscoelastic electrolytes with different polymer concentrations. (A) Electrical model used to fit the Nyquist plot. (B) Bulk and interfacial resistance as a function of polymer concentration in the electrolytes. (C) Warburg element as a function of polymer concentration.



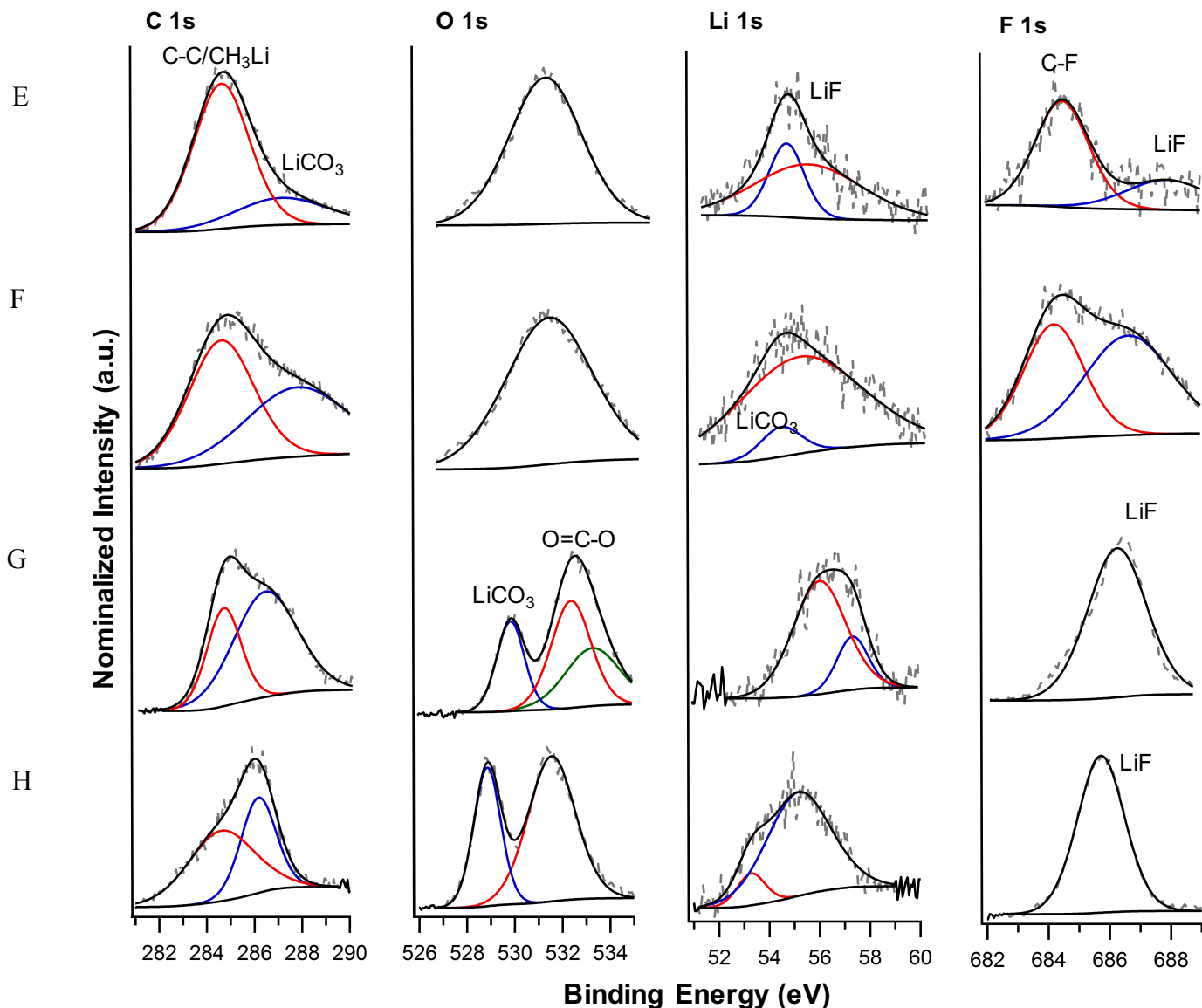
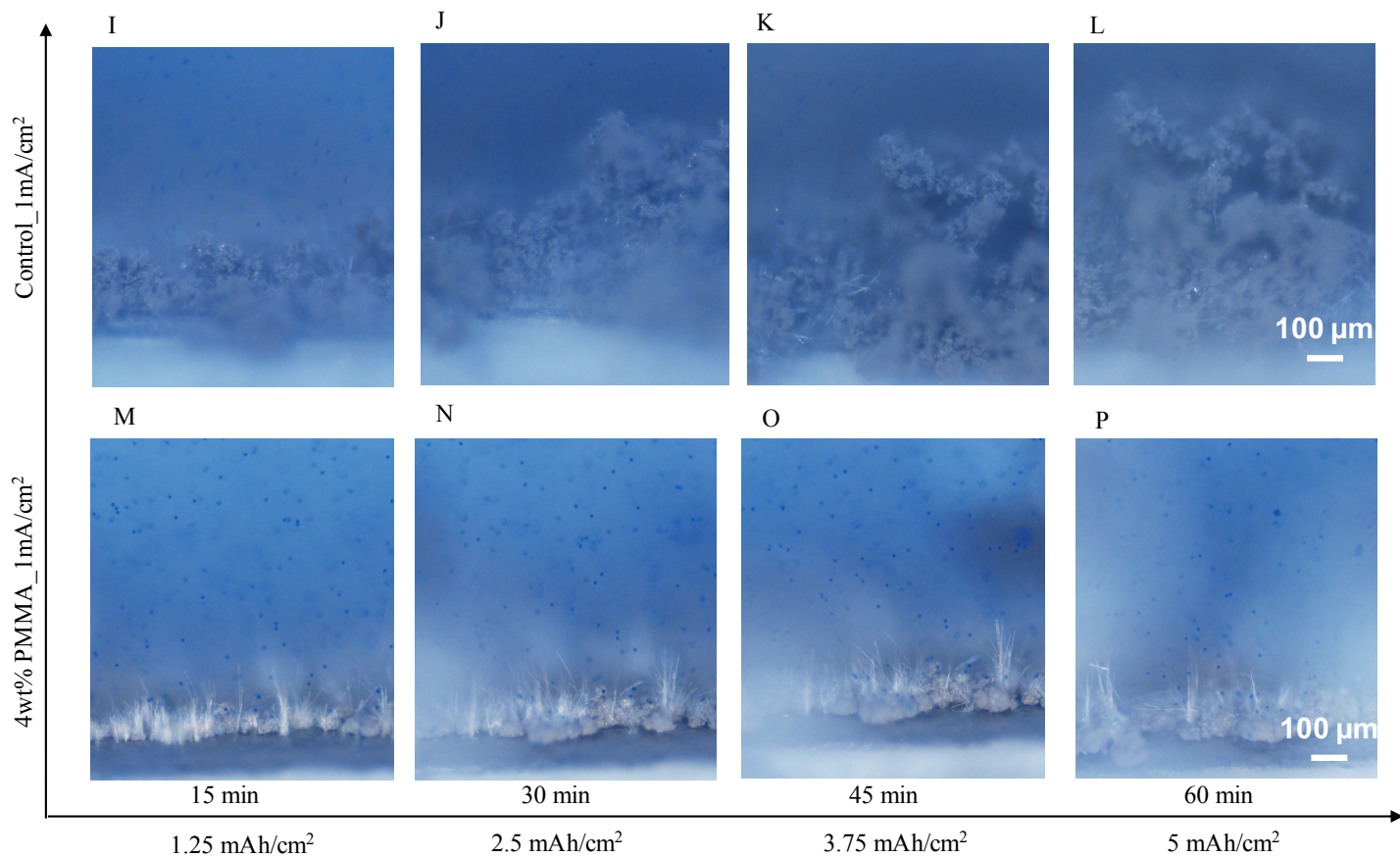
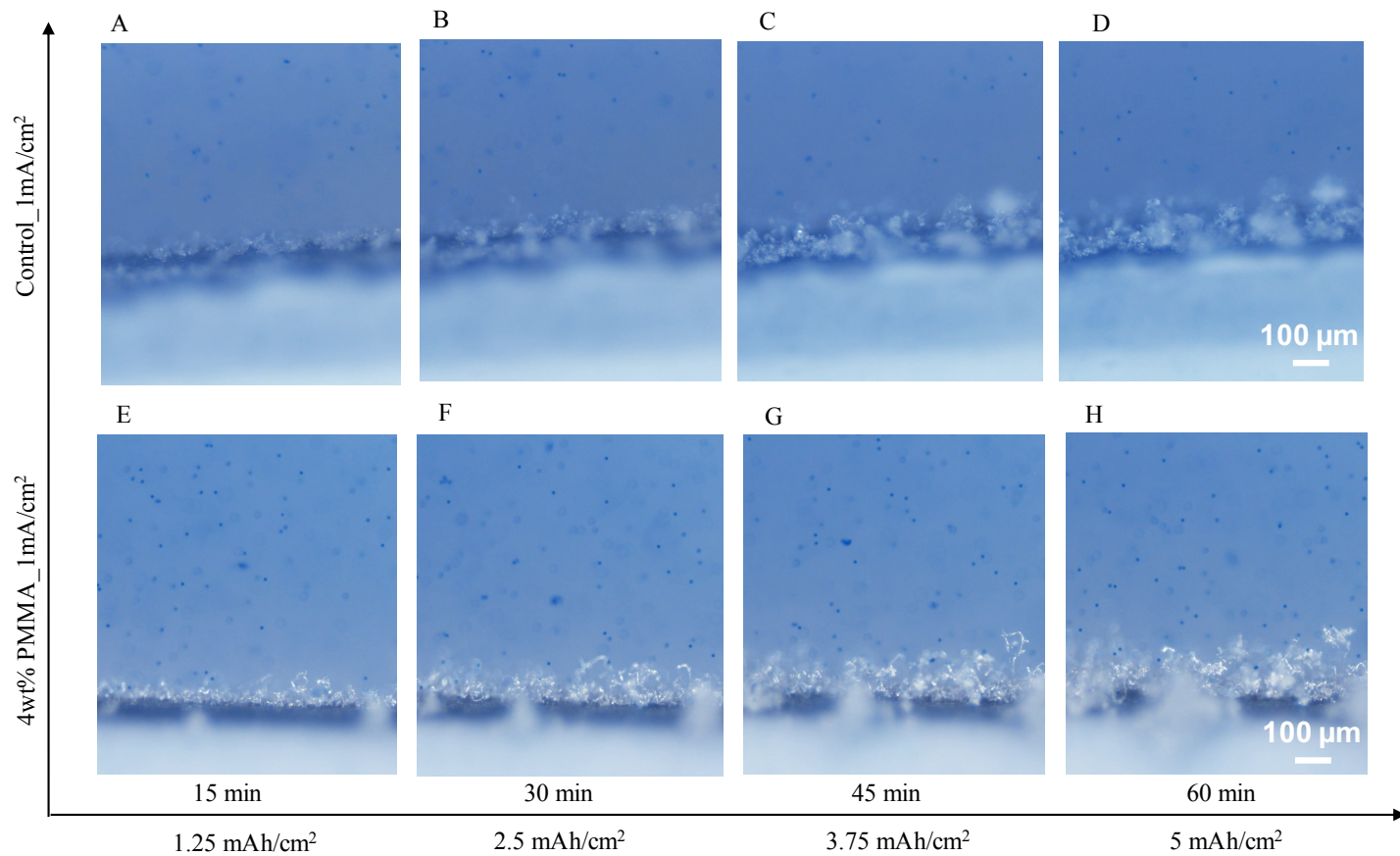


fig. S8. Depth-profiling XPS spectra of a lithium metal surface after electrodeposition for 1 hour at a current density of 1 mA/cm². (A to D) High resolution scan of C 1s, O 1s, Li 1s and F 1s spectra after 0, 30, 1200, 6000s itching by argon with a pass energy of 2 kV and current of 2 μ A in an area of 2x3 mm in the Newtonian liquid electrolyte (EC/PC-1M LiTFSI), indicating an approximate depth of 0 nm, 2.5 nm, 100 nm and 500 nm through the lithium surface. (E to F) High resolution scan of C 1s, O 1s, Li 1s and F 1s after 0, 30, 1200, 6000s itching in the viscoelastic electrolyte (4 wt% PMMA in EC/PC-1 M LiTFSI). The obtained XPS spectra were analyzed by CasaXPS software and calibrated with a hydrocarbon C 1s signal at 284.6 eV.



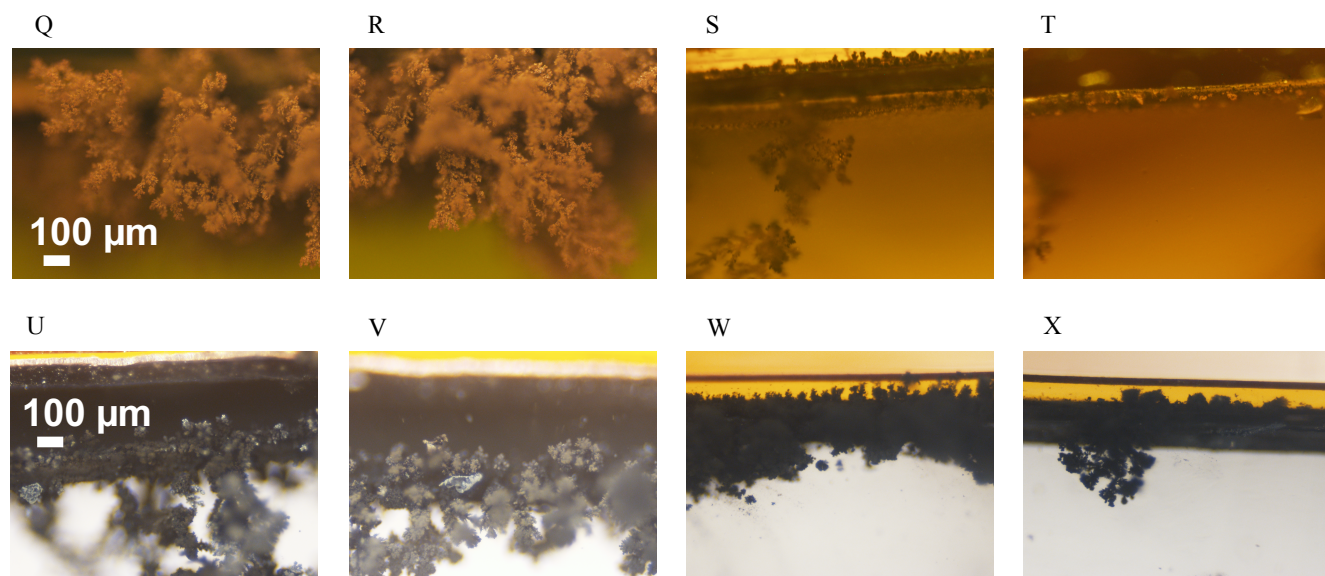


fig. S9. Photographic images showing evolution of various metal electrode/electrolyte interfaces during electrodeposition. Snapshots showing the evolution of a Li electrode at current density of 1 mA/cm^2 . (A to D) results obtained in the control (EC/PC-1M LiTFSI) electrolyte. (E to H) results for the viscoelastic liquid electrolyte (4 wt% PMMA in EC/PC-1 M LiTFSI). Snapshots showing the evolution of a Na electrode at current density 1 mA/cm^2 . (I to L) results obtained in the (EC/PC-1M NaClO_4) control electrolyte. (M to P) results for a viscoelastic liquid electrolyte (4 wt% PMMA in EC/PC-1 M NaClO_4). Copper in (Q and R) the control liquid electrolyte (DMSO-0.12 M CuCl_2) and (S and T) the viscoelastic electrolyte (4 wt% PMMA in DMSO-0.12 M CuCl_2) for one hour at 5 mA/cm^2 . Zinc in (U and V) control liquid electrolyte (DMSO-0.12 M ZnCl_2) and (W and X) the viscoelastic electrolyte (4 wt% PMMA in DMSO-0.12 M ZnCl_2) for one hour at 5 mA/cm^2 .

table S1. Measured Li^+ transference numbers and calculated limiting current densities [in the optical cell (J_1) and O-ring coin cell (J_2)] for electrolytes used in the study.

	t^+	$J_1 \text{ (mA/cm}^2\text{)}$	$J_2 \text{ (mA/cm}^2\text{)}$
Control	0.428	1.50	2.95
1wt% PMMA	0.442	1.58	3.10
4wt% PMMA	0.396	1.32	2.59
8wt% PMMA	0.330	0.97	1.91